Hepatitis B virus X protein targets the Bcl-2 protein CED-9 to induce intracellular Ca^{2+} increase and cell death in *Caenorhabditis elegans*

Xin Geng[a], Brian L. Harry[a,1], Qinghua Zhou[a,1], Riley Robert Skeen-Gaar[a], Xiao Ge[b], Eui Seung Lee[a], Shohei Mitani[c], and Ding Xue[a,b,2]

[a]Department of Molecular, Cellular, and Developmental Biology, University of Colorado, Boulder, CO 80309; [b]School of Life Sciences, Tsinghua University, Beijing 100084, China; and [c]Department of Physiology, Tokyo Women's Medical University, School of Medicine, Tokyo, 162-8666, Japan

Edited* by Xiaodong Wang, University of Texas Southwestern Medical Center, Dallas, TX, and approved September 19, 2012 (received for review March 18, 2012)

HBx is a multifunctional hepatitis B virus (HBV) protein that is crucial for HBV infection and pathogenesis and a contributing cause of hepatocyte carcinogenesis. However, the host targets and mechanisms of action of HBx are poorly characterized. We show here that expression of HBx in *Caenorhabditis elegans* induces both necrotic and apoptotic cell death, mimicking an early event of liver infection by HBV. Genetic and biochemical analyses indicate that HBx interacts directly with the B-cell lymphoma 2 (Bcl-2) homolog CED-9 (cell death abnormal) through a Bcl-2 homology 3 (BH3)-like motif to trigger both cytosolic Ca^{2+} increase and cell death. Importantly, Bcl-2 can substitute for CED-9 in mediating HBx-induced cell killing in *C. elegans*, suggesting that CED-9 and Bcl-2 are conserved cellular targets of HBx. A genetic suppressor screen of HBx-induced cell death has produced many mutations, including mutations in key regulators from both apoptosis and necrosis pathways, indicating that this screen can identify new apoptosis and necrosis genes. Our results suggest that *C. elegans* could serve as an animal model for identifying crucial host factors and signaling pathways of HBx and aid in development of strategies to treat HBV-induced liver disorders.

The hepatitis B virus (HBV) X gene, one of the four coding genes in the HBV genome, encodes a multifunctional protein (HBx) that is essential for HBV infection and replication (1, 2). HBx also affects multiple cellular events in infected cells, including transcription, signal transduction, proteasome activity, cell cycle progression, and cell death (3). HBx has been shown to play an important role in neoplastic transformation of hepatocytes in HBV-infected patients. For example, HBx expression is detected in the majority of patients with HBV-related hepatocellular carcinoma (HCC) and HBx is the most frequently integrated viral sequence found in HCC (4). Moreover, high incidences of liver tumors were found in transgenic mice expressing only HBx, suggesting a causal relationship between HBx and HCC (5–9). How HBx expression in the liver leads to development of HCC is not understood. Adding to the puzzle, HBx binds a vast number of proteins in various in vitro systems, including factors involved in transcription and DNA repair, mitochondria-related proteins, and cell cycle regulators (2, 3). Most of these protein interactions have not been confirmed under conditions that recapitulate HBV infection in hepatocytes. As a result, the actual cellular targets of HBx remain elusive (2, 3).

Many studies have linked HBx expression to the activation of necrosis and apoptosis in hepatocytes. HBx can sensitize liver cells to cell death by various insults, including tumor necrosis factor-α (TNF-α) and growth factor deprivation (10, 11). HBx induces mitochondria aggregation, loss of mitochondrial membrane potential, and cytochrome *c* release, indicating that HBx may act through mitochondria to induce cell death (12–15). Apoptosis and necrosis are also early events of liver pathogenesis in HBx transgenic mice and may lead to development of cirrhosis and HCC (9, 10, 12). Whereas these reports suggest a hepatotoxic function for HBx, the cellular targets and signaling pathways that HBx exploits to promote cell death and the development of HCC remain unclear. It has been hypothesized that chronic hepatocyte cell death causes cycles of inflammatory cytokine release, local liver damage, and compensatory regeneration, leading to the continual acquisition of oncogenic mutations and the development of HCC (10, 16). Therefore, identification of cellular targets and pathways that mediate HBx-induced cell death is critical for treating HBV-related liver disease.

Calcium signaling is central to multiple HBx activities (3). HBx is responsible for triggering cytosolic Ca^{2+} increase in HBV-infected hepatocytes, which is required for HBV DNA replication (17). HBx-induced elevation of cytosolic Ca^{2+} is also important for HBV core assembly (18), some HBx-activated transcriptional events (17, 19), and activation of several signaling cascades, including JNK and MAPK pathways (3). Additionally, HBx has been shown to modulate cell death by altering cytosolic Ca^{2+} (20). Although HBx has been suggested to target mitochondria and mitochondria permeability transition (MPT) in Ca^{2+} regulation (14, 15, 17), the cellular target(s) with which HBx interacts to alter cytosolic Ca^{2+} is unknown and could be at the crux of HBx biology and HBV therapy.

Given the extreme complexity of HBx study in mammals, we used the simple, genetically tractable animal model *Caenorhabditis elegans* to identify HBx targets and signaling pathways. We identified the human Bcl-2 homolog, CED-9, as the cellular target that HBx interacts with to induce cytosolic Ca^{2+} increase and cell killing.

Results

Expression of HBx in *C. elegans* Causes Ectopic Apoptosis and Necrosis. To assess the activities of HBx in *C. elegans*, we induced global expression of HBx under the control of the *C. elegans* heat-shock promoters (P_{hsp}HBx). Expression of HBx in *C. elegans* had deleterious effects, leading to a high percentage of embryonic lethality (Fig. 1 *A* and *B*). Approximately 97% of P_{hsp}HBx transgenic embryos did not hatch and were invariably deformed (Fig. 1 *A* and *B*). Many contained large vacuoles that resembled necrotic cells (Fig. 1*A*, arrowheads) and raised discs characteristic of apoptotic cells (Fig. 1*A*, arrows). To determine the nature of HBx-induced cell death, we introduced the P_{hsp}HBx transgenes into animals defective in *ced-3*, which encodes a caspase essential for apoptosis (21), or animals defective in *mec-6*, which is important for necrosis (22). A strong loss-of-function (*lf*) mutation in *ced-3* (*n2433*) or *mec-6* (*e1342*) partially suppressed embryonic lethality caused by HBx overexpression

Author contributions: X. Geng, B.L.H., Q.Z., and D.X. designed research; X. Geng, B.L.H., Q.Z., and R.R.S.-G. performed research; X. Ge, E.S.L., and S.M. contributed new reagents/analytic tools; X. Geng, B.L.H., Q.Z., and D.X. analyzed data; and X. Geng, B.L.H., X. Ge, and D.X. wrote the paper.

The authors declare no conflict of interest.

*This Direct Submission article had a prearranged editor.

[1]B.L.H. and Q.Z. contributed equally to this work.

[2]To whom correspondence should be addressed. E-mail: ding.xue@colorado.edu.

This article contains supporting information online at www.pnas.org/lookup/suppl/doi:10.1073/pnas.1204652109/-/DCSupplemental.

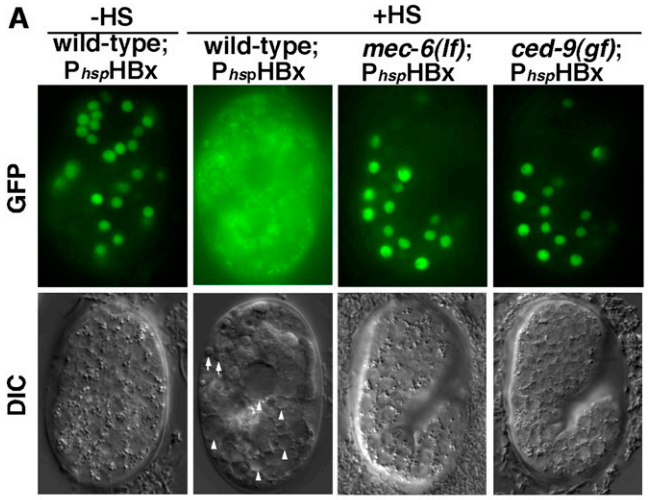

B

Genotype		% Embryo Lethality (+HS)
Wild-type (N2)		20%
N2; Ex(P_{hsp}HBx)	L1	97%
	L2	98%
ced-3(n2433); Ex(P_{hsp}HBx)	L1	51%
	L2	55%
mec-6(e1342); Ex(P_{hsp}HBx)	L1	31%
	L2	36%
ced-9(n1950); Ex(P_{hsp}HBx)	L1	28%
	L2	24%

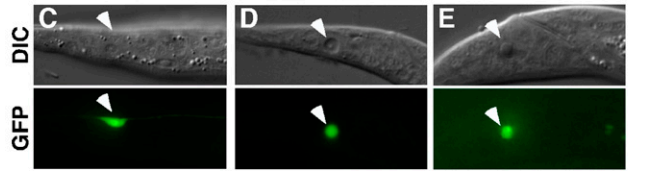

Fig. 1. Induction of both apoptosis and necrosis in *C. elegans* by HBx expression. (*A*) GFP fluorescent and differential interference contrast (DIC) images of embryos transgenic for P_{hsp}HBx and $P_{sur\text{-}5}$SUR-5::GFP before (−HS) and after (+HS) heat-shock treatment. SUR-5::GFP was seen in nuclei of many cells at most developmental stages. (*B*) Suppression of HBx-induced embryonic lethality by a loss-of-function mutation in *ced-3* or *mec-6* or a gain-of-function mutation in *ced-9*. HBx transgenic embryos were heat-shocked at 33 °C for 1 h. Under this heat-shock treatment, 20% of wild-type *C. elegans* embryos did not hatch. L1 and L2 represent two independent extrachromosomal transgenes that were crossed into different mutant backgrounds. At least 300 transgenic embryos were scored for each strain. (*C*–*E*) DIC and GFP images of the PLM neurons. PLM displayed a normal, oval-shape morphology in a *smIs3* animal (*C*). In *smIs98* animals, dying PLM neurons adopted morphology characteristic of necrotic cells (*D*) or apoptotic cells (*E*).

(Fig. 1*B*), indicating that both apoptotic and necrotic cell death contributes to lethality of HBx transgenic embryos.

To better analyze the cell-killing activity of HBx, we expressed HBx in six mechanosensory neurons under the control of the *mec-7* gene promoter ($P_{mec\text{-}7}$HBx) (Fig. S1*A*). To aid in identification of these nonessential neurons, we expressed GFP under the control of the *mec-3* promoter ($P_{mec\text{-}3}$GFP), which drives gene expression in the same six touch cells plus four other sensory neurons (Fig. S1*A*). An integrated transgene (*smIs98*) containing both $P_{mec\text{-}7}$HBx and $P_{mec\text{-}3}$GFP was used to assay killing of touch cells by HBx (Fig. S1*A*). On average, 13–50% of touch cells in *smIs98* animals underwent ectopic cell death, with the two posterior lateral microtubule (PLM) neurons showing most ectopic deaths (50%; Fig. S1*B*). PLM death was thus used in all subsequent genetic analysis. Some dying touch cells in *smIs98* animals displayed an enlarged vacuolar morphology characteristic of necrotic cells (Fig. 1*D*) and some displayed the raised disk-like morphology of apoptotic cells (Fig. 1*E*). Consistently, cell killing by HBx was partially suppressed by either *ced-3*(*n2433*) or *mec-6*(*e1342*) *lf* mutations and eliminated by loss of both genes (Fig. 2*A*). These results confirm that HBx induces both apoptosis and necrosis in *C. elegans*.

Many genes involved in apoptosis and necrosis have been identified in *C. elegans* (Fig. 2*B*) (21, 23). In the apoptotic pathway, four key proteins, EGL-1 [similar to human Bcl-2 homology 3 (BH3)-only pro-apoptotic proteins], CED-9 (human Bcl-2 proteins), CED-4 (human Apaf-1), and CED-3 (human caspases), act sequentially to control activation of apoptosis (21). In the necrotic pathway, several conserved endoplasmic reticulum (ER) proteins involved in regulating Ca^{2+} homeostasis, including two Ca^{2+}-binding proteins, CRT-1 (calrecticulin) and CNX-1 (calnexin), and two Ca^{2+} channels, ITR-1 (inositol trisphosphate receptor) and UNC-68 (uncoordinated, a ryanodine receptor homolog), control release of Ca^{2+} from ER to cytosol in response to various necrotic insults (23). Ca^{2+} elevation in cytosol then initiates necrosis through conserved Ca^{2+}-dependent proteases, CLP-1 (calpain family) and TRA-3 (transformer), and their downstream aspartyl proteases (ASP-3 and ASP-4) (24). We examined whether these key components of apoptotic and necrotic cell death pathways affect HBx-induced cell death. Loss of *egl-1*, *ced-3*, or *ced-4* partially suppressed HBx-induced cell death (from 50% to 22–26% PLM death; Fig. 2*A*), indicating that HBx induces cell death partly through the apoptotic

A

Genotype	% PLM Missing
smIs98	50%
smIs98; ced-3(n2433)	26%
smIs98; ced-4(n1162)	22%
smIs98; egl-1(n3082)	22%
smIs98; ced-9(n1950)	1%
smIs98; ced-4(n1162) ced-9(n2812)	1%
smIs98; mec-6(e1342)	9%
smIs98; clp-1(tm690)	13%
smIs98; tra-3(e1107am)	19%
smIs98; asp-3(tm4559)	12%
smIs98; asp-4(ok2693)	13%
smIs98; itr-1(sa73)	29%
smIs98; unc-68(e540)	50%
smIs98; unc-68(e540); itr-1(sa73)	15%
smIs98; crt-1(bz29)	28%
smIs98; cnx-1(nr2009)	32%
smIs98; cnx-1(nr2009); crt-1(bz29)	14%
smIs98; ced-3(n2433); mec-6(e1342)	3%
smIs98; ced-3(n2433); clp-1(tm690)	3%
smIs98; ced-3(n2433); itr-1(sa73)	5%
smIs98; ced-3(n2433); crt-1(bz29)	5%

B

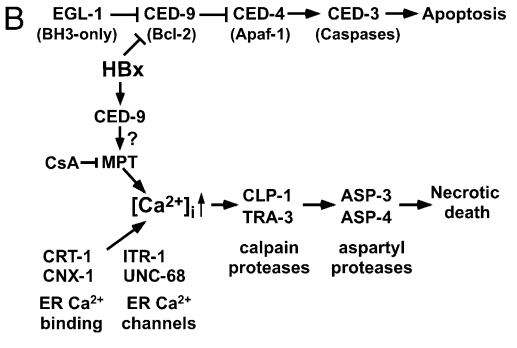

Fig. 2. Components and pathways involved in HBx-induced apoptosis and necrosis in *C. elegans*. (*A*) Cell-killing activity of HBx in various mutants defective in either apoptosis or necrosis or in both. The percentage of PLM death was scored in animals with the indicated genotypes. At least 200 L4 stage larvae from each strain were scored. (*B*) HBx-induced apoptosis and necrosis pathways in *C. elegans*. Key regulators of apoptosis and necrosis in *C. elegans* are shown, with corresponding human homologs (apoptosis) and biochemical properties (necrosis) indicated. $[Ca^{2+}]_i$ indicates cytosolic Ca^{2+} concentration. CsA: cyclosporine A. The position and biochemical function of *mec-6* in necrosis are unknown.

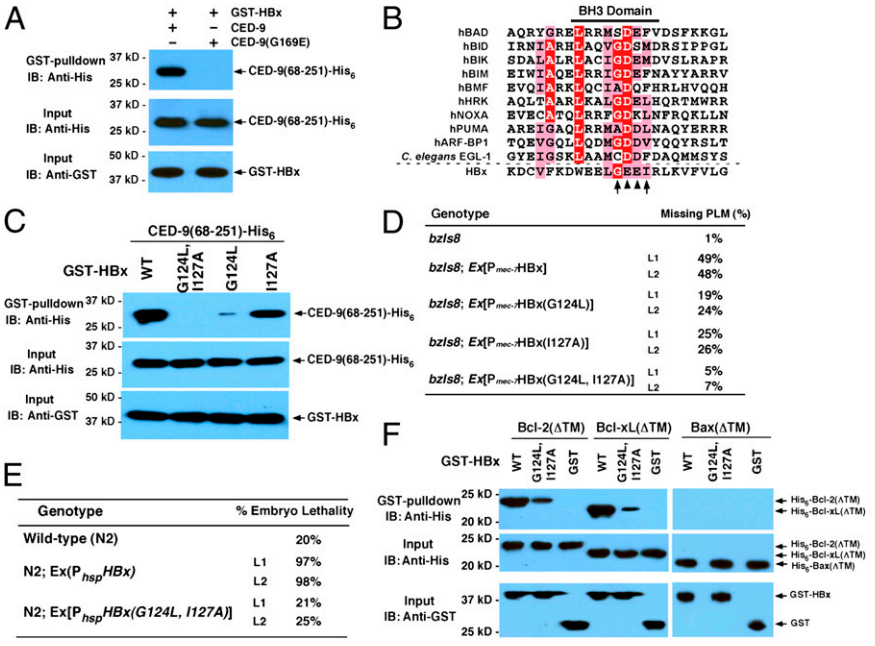

Fig. 3. Association of HBx with CED-9 or Bcl-2 family proteins through the BH3-like motif of HBx. (*A*) Purified GST-HBx (2.5 μg) immobilized on glutathione resins was incubated with 5 μg of CED-9 (68-251)-His_6 or CED-9(68-251; G169E)-His_6. One portion of the incubation mix was analyzed by immunoblotting (IB) to examine the input levels of GST-HBx and CED-9(68-251)-His_6 proteins. The remaining portion was used for the pull-down experiments and the proteins remaining on the resin were resolved on a SDS polyacrylamide gel (SDS/PAGE) and visualized by IB. (*B*) Sequence alignment of the BH3 domains from various pro-apoptotic BH3-only proteins and the BH3-like motif of HBx. Residues that are identical are shaded in red and residues that are similar in pink. Gly124 and Ile127 of HBx are indicated with arrows and Glu125 and Glu126 with arrowheads. (*C*) Binding of CED-9 (68-251)-His_6 to GST-HBx, GST-HBx(G124L), GST-HBx (I127A), or GST-HBx(G124L, I127A). The pull-down assay was carried out as described in *A*. (*D*) Cell-killing activity of the HBx mutants. *bzIs8* is an integrated transgene carrying the $P_{mec\text{-}4}$GFP construct, which directs GFP expression in six touch cells and allows scoring of the PLM cell death. L1 and L2 represent two independent extrachromosomal (Ex) transgenic lines. At least 100 transgenic L4 larvae were scored in each strain. (*E*) Assay of embryonic lethality induced by global expression of HBx or HBx(G124L, I127A) was carried out as described in Fig. 1*B*. Three hundred transgenic embryos were scored for each strain. (*F*) Association of HBx with human Bcl-2 and Bcl-xL proteins. The pull-down assay was carried out as described in *A*, using 2.5 μg of GST-HBx, GST-HBx(G124L, I127A), and GST, and 5 μg recombinant Bcl-2, Bcl-xL, and Bax proteins that were N-terminally tagged with six histidines and without their transmembrane domains (ΔTM).

pathway. Likewise, loss of *crt-1*, *cnx-1*, *itr-1*, *clp-1*, *tra-3*, *asp-3*, or *asp-4* partially suppressed HBx-induced cell killing (from 50% to 12–32% PLM death; Fig. 2*A*), indicating that HBx induces cell death in part through the necrotic pathway. Importantly, loss of *ced-3* and one of the components in the necrotic pathway (*mec-6*, *clp-1*, *itr-1*, and *crt-1*) almost completely blocked ectopic touch cell death induced by HBx (Fig. 2*A*), indicating that apoptosis and necrosis account for virtually all cell death induced by HBx.

CED-9 Is Required for HBx-Induced Cell Death. Like loss of *egl-1*, *ced-4*, or *ced-3*, a gain-of-function (*gf*) mutation (*n1950*) in *ced-9* prevents most somatic apoptosis in *C. elegans* (25). However, unlike *egl-1(lf)*, *ced-4(lf)*, and *ced-3(lf)* mutations that partially block HBx-induced cell death, *ced-9(n1950gf)* completely inhibited HBx-induced touch cell death (Fig. 2*A*) and embryonic lethality (Fig. 1*B*). Moreover, a strong *lf* mutation in *ced-9* (*n2812*) completely suppressed ectopic cell killing induced by HBx in the *ced-4(n1162)* mutant background (Fig. 2*A*), which blocks massive ectopic cell deaths and embryonic lethality caused by *ced-9(n2812)* (25). These results indicate that HBx induces both apoptotic and necrotic cell death through CED-9.

The *ced-9(n1950gf)* mutation results in substitution of Gly^{169} by Glu in the BH3-binding pocket of CED-9, which disrupts the binding of the BH3-only protein EGL-1 to CED-9 and prevents EGL-1–induced release of pro-apoptotic CED-4 from the CED-4/CED-9 complex tethered on the surface of mitochondria (26, 27). We hypothesized that HBx acts by binding to CED-9, thereby antagonizing its death inhibitory function. We tested whether HBx binds CED-9 in vitro, using a GST fusion protein pull-down assay. GST-HBx specifically interacted with CED-9 tagged with a six-histidine epitope but not with the mutant CED-9(G169E) protein (Fig. 3*A*). Interestingly, HBx contains a sequence (residues 116–132) that is distantly related to the BH3 motif of many pro-apoptotic BH3-only proteins (Fig. 3*B*) (28, 29). We tested the possibility that the interaction with CED-9 occurs through this motif by altering two amino acids (Gly^{124} to Leu and Ile^{127} to Ala) in HBx that are conserved among BH3-only proteins (Fig. 3*B*) and that face CED-9 in a structural model of the HBx/CED-9 complex (Fig. 4*A*). G124L substitution markedly reduced and I127A substitution compromised the binding of HBx to CED-9 in vitro (Fig. 3*C*). Alteration of both residues (G124L; I127A) abolished association of HBx with CED-9 (Fig. 3*C*). Consistently, in an in vitro CED-4 releasing assay (27), HBx, but not HBx(G124L; I127A), was able to release CED-4 from the GST-CED-9/CED-4 complexes tethered to Glutathione resin (Fig. S2). When HBx(G124L) or HBx (I127A) was expressed under the control of the *mec-7* promoter, both mutant proteins displayed reduced cell-killing activity, whereas the double mutant, HBx(G124L; I127A), induced minimal ectopic touch cell death (Fig. 3*D*). Similarly, HBx (G124L; I127A) did not cause embryonic lethality in *C. elegans* like HBx when expressed under the control of the heat-shock promoters (Fig. 3*E*). These in vitro and in vivo results indicate that association of HBx with CED-9 is required for HBx to induce ectopic cell killing in *C. elegans*.

To characterize further the interaction between HBx and CED-9, we performed structural modeling of the HBx/CED-9 complex using the published EGL-1/CED-9 complex structure (30), replacing the EGL-1 BH3 helix with the putative BH3 motif of HBx. In the modeled HBx/CED-9 structure, Glu^{125} and Glu^{126} of HBx are in the vicinity of the Gly^{169} residue of CED-9 (Fig. 4*B*). The replacement of Gly^{169} by a bulky, negatively charged Glu in the *ced-9(n1950gf)* mutant is expected to cause a steric clash and/or charge repulsion with either Glu^{125} or Glu^{126} or with both, disrupting the interaction between HBx and CED-9 (Fig. 4*B*). We thus generated two single Glu to Ala substitutions (E125A and E126A) in HBx and tested whether residues with a neutral, smaller side chain may alleviate steric clash or charge repulsion and restore binding of HBx to CED-9(G169E). Although neither mutation affected binding of HBx to wild-type CED-9, E125A, but not E126A, specifically restored binding of HBx to CED-9(G169E) in vitro (Fig. 4*C*). In vivo, both HBx (E125A) and HBx(E126A) caused ectopic touch cell death and a high percentage of embryonic lethality in wild-type animals like HBx when expressed under the control of the *mec-7* and the heat-shock promoters, respectively (Fig. 4 *D* and *E*). However, only HBx(E125A), but not HBx or HBx(E126A), induced robust killing of touch cells and embryos in *ced-9(n1950)* animals (Fig. 4 *D* and *E*). These results correlate with the observation that HBx (E125A), but not HBx or HBx(E126A), bound CED-9(G169E) in

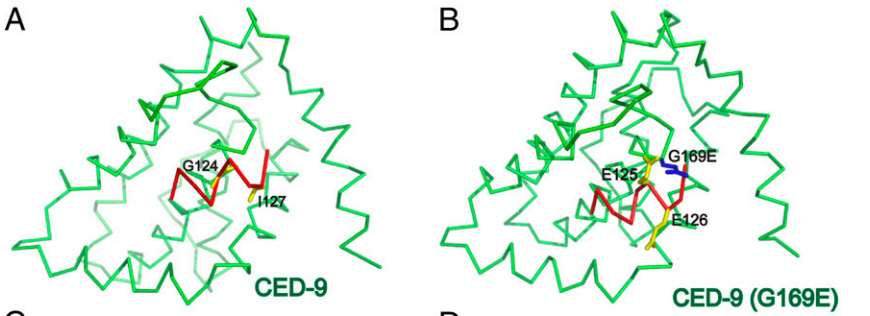

C

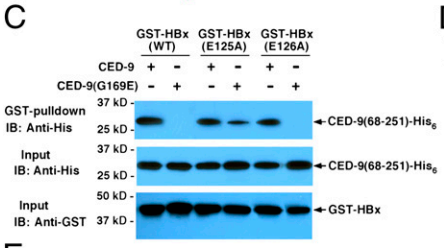

D

Genotype		Missing PLM (%)
bzIs8		1%
ced-9(n1950); bzIs8		0%
bzIs8; Ex[P$_{mec-7}$HBx]	L1	49%
	L2	48%
bzIs8; Ex[P$_{mec-7}$HBx(E125A)]	L1	47%
	L2	49%
bzIs8; Ex[P$_{mec-7}$HBx(E126A)]	L1	51%
	L2	47%
ced-9(n1950); bzIs8; Ex[P$_{mec-7}$HBx]	L1	0%
	L2	1%
ced-9(n1950); bzIs8; Ex[P$_{mec-7}$HBx(E125A)]	L1	48%
	L2	39%
ced-9(n1950); bzIs8; Ex[P$_{mec-7}$HBx(E126A)]	L1	1%
	L2	1%

E

Genotype		% Embryo Lethality
Wild-type (N2)		20%
N2; Ex(P$_{hsp}$HBx)	L1	97%
	L2	98%
N2; Ex[P$_{hsp}$HBx(E125A)]	L1	96%
	L2	95%
N2; Ex[P$_{hsp}$HBx(E126A)]	L1	98%
	L2	96%
ced-9(n1950); Ex(P$_{hsp}$HBx)	L1	28%
	L2	24%
ced-9(n1950); Ex[P$_{hsp}$HBx(E125A)]	L1	89%
	L2	90%
ced-9(n1950); Ex[P$_{hsp}$HBx(E126A)]	L1	22%
	L2	27%

F

Genotype		Missing PLM (%)
smIs98; ced-9(n1950)		1%
smIs98; ced-9(n1950) ; Ex[P$_{mec-7}$CED-9]	L1	52%
	L2	49%
	L3	46%
smIs98; ced-9(n1950) ; Ex[P$_{mec-7}$hBcl-2]	L1	44%
	L2	41%
	L3	39%
smIs98; ced-9(n1950) ; Ex[P$_{mec-7}$CED-9ΔTM]	L1	9%
	L2	7%

Fig. 4. Restoration of HBx binding to CED-9(G169E) and cell killing in *ced-9(n1950)* animals by a designed compensatory mutation in HBx. (*A*) Ribbon stereo-drawing of a modeled complex structure between the BH3-like domain of HBx (residues 120–128, in red) and CED-9 (in green). The BH3-like peptide of HBx interacts with CED-9 through the same interface as that of the BH3 peptide of EGL-1 (*Materials and Methods*). The two conserved residues (Gly124 and Ile127) in HBx facing the interface are shown in yellow. (*B*) A modeled complex structure between the BH3-like domain of HBx (in red) and CED-9(G169E) (in green), in which Glu replaces Gly169 (in blue). The larger, negatively charged side chain of Glu169 in CED-9 may cause steric clash or charge repulsion or both with two residues in HBx in the vicinity, Glu125 and Glu126 (in yellow). (*C*) Restoration of HBx binding to CED-9(G169E) by Glu125 to Ala substitution in HBx. Five micrograms of CED-9(68-251)-His$_6$ or CED-9 (68-251, G169E)-His$_6$ was incubated with 2.5 μg of GST-HBx, GST-HBx(E125A), or GST-HBx(E126A) immobilized on glutathione resins. The pull-down assay was performed as described in Fig. 3*A*. (*D*) Induction of PLM death in *ced-9(n1950)* animals by HBx(E125A). L1 and L2 represent two independent *bzIs8* or *ced-9 (n1950); bzIs8* transgenic lines carrying a wild-type or a mutant P$_{mec-7}$HBx construct. At least 100 transgenic L4 larvae from each line were scored. (*E*) Embryonic lethality caused by global expression of HBx(E125A) in *ced-9(n1950)* animals. L1 and L2 represent two independent wild-type or *ced-9(n1950)* transgenic lines carrying wild-type or mutant P$_{hsp}$HBx constructs. Three hundred transgenic embryos were scored. (*F*) Restoration of HBx cell killing in *ced-9(n1950)* animals by expression of *ced-9* or human Bcl-2. L1–L3 represent independent *ced-9(n1950); smIs98* transgenic lines carrying P$_{mec-7}$CED-9, P$_{mec-7}$hBcl-2, or P$_{mec-7}$CED-9ΔTM. At least 50 transgenic L4 larvae from each line were scored.

vitro (Fig. 4*C*). Together, they provide strong evidence that HBx induces cell death in *C. elegans* by directly interacting with CED-9.

Bcl-2 Can Substitute for CED-9 in Mediating HBx-Induced Cell Death. The functions of CED-9 and Bcl-2 in cell death regulation are highly conserved, and Bcl-2 can partially substitute for *ced-9* to inhibit apoptosis in *C. elegans* (25). Therefore, we tested whether HBx binds Bcl-2 family proteins and whether Bcl-2 can substitute for CED-9 in mediating HBx-induced cell killing in *C. elegans*. We found that GST-HBx specifically interacted with human anti-apoptotic proteins Bcl-2 and Bcl-xL, but not with the pro-apoptotic protein Bax (Fig. 3*F*). The binding of HBx to Bcl-2 and Bcl-xL was markedly reduced by the G124L and I127A mutations, indicating that HBx also interacts with Bcl-2 and Bcl-xL in vitro through its BH3-like motif.

HBx was unable to induce touch cell death in *ced-9(n1950)* animals owing to its inability to bind CED-9(G169E) (Figs. 2*A* and 3*A*). This suppression of HBx-induced cell death was completely reversed by expression of wild-type CED-9 (P$_{mec-7}$CED-9) in *smIs98*; *ced-9(n1950)* animals (Fig. 4*F*). Importantly, expression of human Bcl-2 in touch cells (P$_{mec-7}$hBcl-2) also completely restored HBx-induced cell killing in *smIs98*; *ced-9(n1950)* animals (Fig. 4*F*), indicating that HBx interactions with Bcl-2 and CED-9 and the ensuing signaling mechanisms are conserved.

HBx Targets CED-9 to Induce Cytosolic Ca^{2+} Increase. Because HBx acts through CED-9 to induce necrosis and because cytosolic Ca^{2+} increase is essential for activation of necrosis in *C. elegans* (23), we examined whether HBx targets CED-9 to affect intracellular Ca^{2+}. A *C. elegans* strain carrying an integrated transgene (*bzIs17*) that expresses a cameleon Ca^{2+} sensor under the control of the *mec-4* gene promoter was used to monitor intracellular Ca^{2+} in touch cells through the fluorescence-resonance energy transfer (FRET) assay (31, 32). In this assay, the FRET ratio (defined as the fluorescence intensity in the FRET channel divided by the intensity in the CFP channel) is indicative of relative cytosolic Ca^{2+} concentrations (32). We first treated *bzIs17* animals with thapsigargin, which inhibits the ER ATPase that pumps Ca^{2+} from the cytosol into the ER and is expected to result in elevation of cytosolic Ca^{2+}. Indeed, the FRET ratio in PLM neurons of thapsigargin-treated animals was significantly higher than that of untreated or vector-treated animals (Fig. 5*A*). To assess the impact of HBx expression on cytosolic Ca^{2+} in living cells, we used the *asp-3(tm4559)* mutation to block most of the touch cell deaths (from 50% missing PLMs to 12%; Fig. 2*A*) induced by an integrated P$_{mec-7}$HBx transgene (*smIs451*). Loss of *asp-3* on its own did not alter cytosolic Ca^{2+}, as the FRET ratios of *bzIs17* and *bzIs17; asp-3(tm4559)* animals were almost identical (Fig. 5*B*). However, in *bzIs17; asp-3(tm4559); smIs451* animals, we observed a 40% increase in the FRET ratio (Fig. 5*B*), indicating that HBx expression in touch cells caused a significant increase in cytosolic Ca^{2+}. Importantly, the HBx-induced Ca^{2+} increase was obliterated by the *ced-9(n1950)* mutation (Fig. 5*B*), which prevents HBx binding to CED-9 (Fig. 3*A*). Therefore, HBx directly targets CED-9 to induce cytosolic Ca^{2+} increase in *C. elegans*.

Mitochondrial Permeability Transition Is Likely Critical to HBx-Induced Ca^{2+} Increase and Necrosis. CED-9 localizes to the outer membrane of mitochondria through its C-terminal transmembrane (TM) domain (26, 33, 34). A CED-9 mutant (CED-9ΔTM) lacking this TM domain fails to localize to mitochondria and is found in the cytoplasm (34). Interestingly, expression of CED-9ΔTM still partially rescues defects in apoptosis and embryonic lethality in *ced-9(lf)* animals (34), indicating that mitochondrial localization is not essential for CED-9 to inhibit apoptosis in *C. elegans* (34). Expression of CED-9ΔTM in touch cells (P$_{mec-7}$CED-9ΔTM) restored PLM

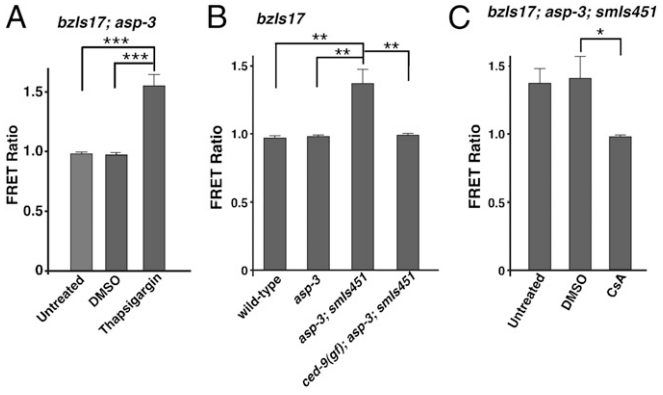

Fig. 5. HBx targets CED-9 to induce cytosolic Ca^{2+} elevation. (*A*) Treatment of *bzIs17; asp-3(tm4559)* animals with 10 μM thapsigargin increased cytosolic Ca^{2+} (indicated by FRET ratio) in PLM neurons (*Materials and Methods*). Untreated or dimethyl sulfoxide (DMSO)-treated animals were assayed as negative controls. (*B*) Expression of HBx in touch cells from an integrated $P_{mec\text{-}7}$HBx transgene (*smIs451*) increased the FRET ratio in PLM neurons of *bzIs17; asp-3(tm4559)* animals. This increase was abolished by the *ced-9 (n1950)* mutation. The FRET ratios were assayed as in *A*. (*C*) Inhibition of HBx-induced cytosolic Ca^{2+} increase by CsA. The FRET ratio of *bzIs17; asp-3 (tm4559); smIs451* animals treated with DMSO or 1 mM CsA was assayed. The *y* axis represents average FRET ratio in PLM neurons and error bars represent SEM. For each strain, at least 15 neurons were assayed. The significance of differences between different strains was determined by an unpaired *t* test. $*P < 0.05$; $**P < 0.005$; $***P < 0.0001$.

killing in *smIs98*; *ced-9(n1950)* animals only to 7–9%, compared with 46–52% PLM killing caused by expression of wild-type CED-9 (Fig. 4*F*). These results indicate that mitochondrial localization is critical for CED-9 to mediate HBx-induced cell killing.

Because MPT has been implicated in mediating HBx-induced Ca^{2+} increase (15, 17), we tested whether MPT affects HBx-induced cell killing and Ca^{2+} increase in *C. elegans*. We first treated *smIs98* animals with cyclosporin A (CsA), a peptide that desensitizes MPT by inhibiting the activity of the mitochondrial cyclophilin D, the essential regulatory component of MPT (35). In *smIs98* animals that normally lost 50% of PLM neurons, CsA treatment reduced the percentage of missing PLMs to 15% (Fig. S1*C*). Similarly, a deletion mutation (*tm4171*) in *cyn-1*, which encodes the *C. elegans* cyclophilin D homolog, reduced the percentage of missing PLMs in *smIs98* animals to 17% (Fig. S1*C*). These results indicate that MPT is likely involved in HBx-induced cell killing. Moreover, loss of *ced-3* enhanced suppression of HBx-induced cell killing by CsA (from 15% PLM death in CsA-treated animals to 4% PLM death; Fig. S1*C*), whereas loss of either *clp-1* or *mec-6* did not (Fig. S1*C*). These results indicate that MPT is critical for HBx-induced necrotic cell death in *C. elegans*.

We then examined whether MPT is involved in HBx-induced cytosolic Ca^{2+} increase. The FRET ratio of *bzIs17; asp-3 (tm4559); smIs451* animals treated with CsA was reduced to the level seen in *bzIs17; asp-3(tm4559)* animals (Fig. 5*C*), indicating that HBx-induced cytosolic Ca^{2+} increase was completely suppressed by CsA. Therefore, HBx-induced Ca^{2+} increase is likely mediated by MPT, which is consistent with observations from human cells (15, 17).

HBx Suppressor Screen Identified Genes Involved in Apoptosis and Necrosis. To identify targets or effectors of HBx-induced cell killing, we conducted a genetic screen to isolate suppressors of the embryonic lethality phenotype caused by global expression of HBx (Fig. 1*B*). To facilitate identification of true HBx suppressors, we performed the screen in *smIs98* animals that coexpressed HBx and GFP under the control of the heat-shock promoters (P_{hsp}HBx and P_{hsp}GFP; Fig. S3*A*). P_{hsp}GFP was used to eliminate mutations that affected transcription from the heat-shock promoters, whereas *smIs98* provided a secondary screen for true suppressors of HBx-induced cell killing. From a screen of ~20,000 haploid genomes, we isolated 31 HBx-induced death suppressors, which were named *hids* mutations. Most *hids* mutations not only suppressed embryonic lethality caused by global expression of HBx but also reduced or blocked ectopic neuronal death in *smIs98* animals (Fig. S3*B*), suggesting that they affect either the apoptotic or the necrotic pathway or both (Fig. S3*B*). Indeed, one mutation (*sm250*) failed to complement *clp-1(tm690)* and is a nonsense allele of *clp-1* (Trp^{295} to Opal). Another *hids* mutation (*sm221*) failed to complement *mec-6 (e1342)* and is a missense allele of *mec-6* (Gly^{77} to Ser). The third *hids* mutant (*sm224*) had no apoptotic cell corpse and carries a nonsense allele of *ced-4* (Glu^{383} to Ochre). These findings indicate that our genetic screen successfully identifies genes involved in HBx-induced apoptosis and necrosis and is a powerful tool to identify new apoptosis and necrosis genes and additional effectors or targets of HBx.

Discussion

HBV infects more than 350 million people and is the leading cause of liver disease and HCC worldwide. As the key pathogenic and oncogenic protein encoded by HBV, HBx presumably interacts with host factors to promote virus replication and various pathogenic consequences, such as liver cell death and HCC (1, 3). However, the host targets of HBx and its mechanisms of action remain elusive, partly due to the lack of a suitable animal model amenable to genetic analysis, inconsistencies often associated with cell culture studies, and the genetic complexity of mammalian systems (e.g., mammals have at least six Bcl-2–like cell death inhibitors). These technical hurdles have prevented definitive identification of HBx cellular targets in the last three decades. Therefore, development of a simpler animal model where HBx host factors and downstream effectors can be identified and verified through powerful molecular genetic approaches becomes imperative for understanding HBx functions and treating HBV patients. In this study, we show that *C. elegans*, with its much simpler genome (only one Bcl-2 homolog) and powerful genetic tools, presents one such animal model. Our finding that expression of HBx in *C. elegans* induces both apoptosis and necrosis, which mimics one of the early cellular events following liver infection by HBV (2, 9, 10, 36), leads to systematic genetic dissection of HBx-induced cell death pathways that involve highly conserved cell death regulators and executors (Fig. 2*B*). These include key regulators of apoptosis (CED-9, CED-4, and CED-3) and critical components in the necrosis pathway, especially those involved in regulating Ca^{2+} signaling, including ER Ca^{2+}-binding proteins and channels (CRT-1, CNX-1, UNC-68, and ITR-1), Ca^{2+}-dependent proteases (CLP-1 and TRA-3), and MPT, many of which previously have not been implicated in HBV or HBx-induced pathogenesis. MPT, however, has been implicated in HBx-induced cell killing and HBV replication in humans (13–15, 17). CED-9, a key apoptosis regulator, was discovered unexpectedly to be a host target of HBx in cell death and Ca^{2+} signaling in *C. elegans*, which led to identification of human Bcl-2 proteins as conserved host targets of HBx-mediated Ca^{2+} stimulation and HBV replication in human hepatocytes (companion article, ref. 37). These findings demonstrate the validity of the *C. elegans* model for studying HBV and HBx. The HBx suppressor screen has identified important regulators of both cell death pathways and still has the potential to identify new targets or effectors of HBx as well as new apoptosis and necrosis genes.

Importantly, the cell-killing activity of HBx is completely dependent on CED-9, a Bcl-2 homolog and a key cell death inhibitor, because a gain-of-function mutation (G169E) in the BH3-binding pocket of CED-9 completely blocks HBx-induced cell death in *C. elegans*. In vitro, HBx interacts with CED-9, but not with CED-9(G169E), through its BH3-like motif. Alteration of two conserved residues in the BH3-like motif of HBx abolishes binding of HBx to CED-9 and HBx's cell-killing activity. A compensatory mutation (E125A) in the BH3-like motif of HBx that restores binding of HBx to CED-9(G169E) allows HBx to kill efficiently in *ced-9(n1950gf)* animals. These in vitro and in

vivo results establish that HBx interacts directly with CED-9 through its BH3-like motif to induce cell killing and that CED-9 is the bona fide cellular target of HBx. Importantly, HBx interacts with Bcl-2 and Bcl-xL, two human anti-apoptotic CED-9 homologs, through the same BH3-like motif in human hepatocytes and this interaction is critical for HBx-induced cytosolic Ca^{2+} elevation, cell death, and HBV viral replication (companion article, ref. 37). These results and the finding that Bcl-2 can fully substitute for CED-9 in *C. elegans* to mediate HBx-induced cell killing suggest that HBx acts through conserved host targets (Bcl-2 family members) and conserved signaling pathways to induce cytosolic Ca^{2+} elevation, cell killing, and other cellular and viral events. They also demonstrate the unique advantage of the *C. elegans* genetic system for unambiguous determination of in vivo protein interaction and target identification, a daunting task in complex mammalian systems.

One central signaling event associated with HBx expression in hepatocytes is elevation of cytosolic Ca^{2+}, which is critical for HBV replication, transcription, and core assembly and is involved in activation of cell death and several other signaling pathways (2, 3). Although the cellular target of HBx-mediated calcium stimulation is unknown, HBx has been proposed to target mitochondria to effect permeability transition (13–15, 17), which plays an important role in regulating intracellular Ca^{2+} homeostasis (38). In this study, we show that HBx interacts directly with CED-9, a mitochondrial protein, to increase cytosolic Ca^{2+}, which then triggers activation of necrosis in *C. elegans* through Ca^{2+}-dependent proteases (CLP-1 and TRA-3) (Figs. 2 and 5). Importantly, CED-9–dependent Ca^{2+} elevation and necrosis induced by HBx can both be suppressed by CsA, an inhibitor of MPT. These results are consistent with the observations in human cells that HBx acts through MPT to control intracellular calcium, cell death, and HBV replication (13–15, 17) and indicate that CED-9 is the cellular target of HBx in elevating intracellular Ca^{2+} (Fig. 2*B*). Because Bcl-2 associates with HBx in HBV-infected hepatocytes (companion article, ref. 37), can substitute for CED-9 in mediating HBx-induced cell killing in *C. elegans*, and has been implicated in regulating MPT (39), Bcl-2 and Bcl-xL, both of which are mitochondrial proteins, are likely targeted by HBx during HBV infection to alter Ca^{2+} signaling. The induced cytosolic Ca^{2+} increase then triggers activation of multiple viral and host events, including HBV replication, assembly, and cell death. Therefore, targeting the BH3-like motif of HBx to prevent HBx binding to Bcl-2 family proteins could be an effective therapeutic strategy for treating HBV-related liver disorders without perturbing host cell-signaling pathways.

Materials and Methods

Maintenance of *C. elegans* strains, cell death assays, generation of transgenic animals, and GST fusion pull-down assays were carried out as described previously (40). Calcium imaging was performed using a *C. elegans* strain with an integrated $P_{mec\text{-}4}$YC2.12 cameleon transgene (*bzIs17*) by the FRET microscopy (31).

Detailed methods and protocols can be found in *SI Materials and Methods*.

ACKNOWLEDGMENTS. We thank X. Gao for help with structural modeling, M. Driscoll for strains, A. Palmer and R. Kerr for suggestions on calcium sensing, T. Blumenthal and R. Garcea for comments on the manuscript, L. P. Ting, P. J. Chen, T. F. Tsai, Y. C. Wu, N. S. Xia, and Q. Yuan for discussions. This work was supported by National Institutes of Health fellowship F30 NS070596 (to B.L.H.) and R01 Grants GM59083, GM79097, and GM088241 (to D.X.).

1. Kremsdorf D, Soussan P, Paterlini-Brechot P, Brechot C (2006) Hepatitis B virus-related hepatocellular carcinoma: Paradigms for viral-related human carcinogenesis. *Oncogene* 25(27):3823–3833.
2. Ganem D, Schneider RJ (2001) The molecular biology of the hepatitis B viruses. *Fields Virology*, eds Knipe DM, et al. (Lippincott Williams & Wilkins, Philadelphia, PA), 4th Ed, Vol 2, pp 2923–2970.
3. Bouchard MJ, Schneider RJ (2004) The enigmatic X gene of hepatitis B virus. *J Virol* 78 (23):12725–12734.
4. Feitelson MA, Duan LX (1997) Hepatitis B virus X antigen in the pathogenesis of chronic infections and the development of hepatocellular carcinoma. *Am J Pathol* 150(4): 1141–1157.
5. Kim CM, Koike K, Saito I, Miyamura T, Jay G (1991) HBx gene of hepatitis B virus induces liver cancer in transgenic mice. *Nature* 351(6324):317–320.
6. Slagle BL, Lee TH, Medina D, Finegold MJ, Butel JS (1996) Increased sensitivity to the hepatocarcinogen diethylnitrosamine in transgenic mice carrying the hepatitis B virus X gene. *Mol Carcinog* 15(4):261–269.
7. Terradillos O, et al. (1997) The hepatitis B virus X gene potentiates c-myc-induced liver oncogenesis in transgenic mice. *Oncogene* 14(4):395–404.
8. Yu DY, et al. (1999) Incidence of hepatocellular carcinoma in transgenic mice expressing the hepatitis B virus X-protein. *J Hepatol* 31(1):123–132.
9. Wu BK, et al. (2006) Blocking of G1/S transition and cell death in the regenerating liver of Hepatitis B virus X protein transgenic mice. *Biochem Biophys Res Commun* 340(3):916–928.
10. Pollicino T, Terradillos O, Lecoeur H, Gougeon ML, Buendia MA (1998) Pro-apoptotic effect of the hepatitis B virus X gene. *Biomed Pharmacother* 52(9):363–368.
11. Su F, Schneider RJ (1997) Hepatitis B virus HBx protein sensitizes cells to apoptotic killing by tumor necrosis factor alpha. *Proc Natl Acad Sci USA* 94(16):8744–8749.
12. Terradillos O, et al. (2002) The hepatitis B virus X protein abrogates Bcl-2-mediated protection against Fas apoptosis in the liver. *Oncogene* 21(3):377–386.
13. Shirakata Y, Koike K (2003) Hepatitis B virus X protein induces cell death by causing loss of mitochondrial membrane potential. *J Biol Chem* 278(24):22071–22078.
14. Clippinger AJ, Gearhart TL, Bouchard MJ (2009) Hepatitis B virus X protein modulates apoptosis in primary rat hepatocytes by regulating both NF-kappaB and the mitochondrial permeability transition pore. *J Virol* 83(10):4718–4731.
15. Rahmani Z, Huh KW, Lasher R, Siddiqui A (2000) Hepatitis B virus X protein colocalizes to mitochondria with a human voltage-dependent anion channel, HVDAC3, and alters its transmembrane potential. *J Virol* 74(6):2840–2846.
16. Sakurai T, et al. (2008) Hepatocyte necrosis induced by oxidative stress and IL-1 alpha release mediate carcinogen-induced compensatory proliferation and liver tumorigenesis. *Cancer Cell* 14(2):156–165.
17. Bouchard MJ, Wang LH, Schneider RJ (2001) Calcium signaling by HBx protein in hepatitis B virus DNA replication. *Science* 294(5550):2376–2378.
18. Choi Y, Gyoo Park S, Yoo JH, Jung G (2005) Calcium ions affect the hepatitis B virus core assembly. *Virology* 332(1):454–463.
19. Lara-Pezzi E, Armesilla AL, Majano PL, Redondo JM, López-Cabrera M (1998) The hepatitis B virus X protein activates nuclear factor of activated T cells (NF-AT) by a cyclosporin A-sensitive pathway. *EMBO J* 17(23):7066–7077.
20. Chami M, Ferrari D, Nicotera P, Paterlini-Bréchot P, Rizzuto R (2003) Caspase-dependent alterations of Ca2+ signaling in the induction of apoptosis by hepatitis B virus X protein. *J Biol Chem* 278(34):31745–31755.
21. Horvitz HR (1999) Genetic control of programmed cell death in the nematode Caenorhabditis elegans. *Cancer Res* 59(7, Suppl):1701s–1706s.
22. Chelur DS, et al. (2002) The mechanosensory protein MEC-6 is a subunit of the C. elegans touch-cell degenerin channel. *Nature* 420(6916):669–673.
23. Driscoll M, Gerstbrein B (2003) Dying for a cause: Invertebrate genetics takes on human neurodegeneration. *Nat Rev Genet* 4(3):181–194.
24. Syntichaki P, Xu K, Driscoll M, Tavernarakis N (2002) Specific aspartyl and calpain proteases are required for neurodegeneration in C. elegans. *Nature* 419(6910):939–944.
25. Hengartner MO, Horvitz HR (1994) C. elegans cell survival gene ced-9 encodes a functional homolog of the mammalian proto-oncogene bcl-2. *Cell* 76(4):665–676.
26. Chen F, et al. (2000) Translocation of C. elegans CED-4 to nuclear membranes during programmed cell death. *Science* 287(5457):1485–1489.
27. Parrish J, Metters H, Chen L, Xue D (2000) Demonstration of the in vivo interaction of key cell death regulators by structure-based design of second-site suppressors. *Proc Natl Acad Sci USA* 97(22):11916–11921.
28. Lu YW, Chen WN (2005) Human hepatitis B virus X protein induces apoptosis in HepG2 cells: Role of BH3 domain. *Biochem Biophys Res Commun* 338(3):1551–1556.
29. Adams JM, Cory S (2007) Bcl-2-regulated apoptosis: Mechanism and therapeutic potential. *Curr Opin Immunol* 19(5):488–496.
30. Yan N, et al. (2004) Structural, biochemical, and functional analyses of CED-9 recognition by the proapoptotic proteins EGL-1 and CED-4. *Mol Cell* 15(6):999–1006.
31. Suzuki H, et al. (2003) In vivo imaging of C. elegans mechanosensory neurons demonstrates a specific role for the MEC-4 channel in the process of gentle touch sensation. *Neuron* 39(6):1005–1017.
32. Palmer AE, Tsien RY (2006) Measuring calcium signaling using genetically targetable fluorescent indicators. *Nat Protoc* 1(3):1057–1065.
33. Pourkarimi E, Greiss S, Gartner A (2012) Evidence that CED-9/Bcl2 and CED-4/Apaf-1 localization is not consistent with the current model for C. elegans apoptosis induction. *Cell Death Differ* 19(3):406–415.
34. Tan FJ, Fire AZ, Hill RB (2007) Regulation of apoptosis by C. elegans CED-9 in the absence of the C-terminal transmembrane domain. *Cell Death Differ* 14(11):1925–1935.
35. Azzolin L, et al. (2010) The mitochondrial permeability transition from yeast to mammals. *FEBS Lett* 584(12):2504–2509.
36. Guo JT, et al. (2000) Apoptosis and regeneration of hepatocytes during recovery from transient hepadnavirus infections. *J Virol* 74(3):1495–1505.
37. Geng X, et al. (2012) Hepatitis B virus X protein targets Bcl-2 proteins to increase intracellular calcium, required for virus replication and cell death induction. *Proc Natl Acad Sci USA* 109:18471–18476.
38. Bernardi P, Rasola A (2007) Calcium and cell death: The mitochondrial connection. *Subcell Biochem* 45:481–506.
39. Breckenridge DG, Xue D (2004) Regulation of mitochondrial membrane permeabilization by BCL-2 family proteins and caspases. *Curr Opin Cell Biol* 16(6):647–652.
40. Geng X, et al. (2008) Inhibition of CED-3 zymogen activation and apoptosis in Caenorhabditis elegans by caspase homolog CSP-3. *Nat Struct Mol Biol* 15(10):1094–1101.

Supporting Information

Geng et al. 10.1073/pnas.1204652109

SI Materials and Methods

Worm Strains and Culture Conditions. *Caenorhabditis elegans* strains were cultured at 20 °C, using standard procedures (1). The N2 Bristol strain was used as the wild-type strain. The following alleles were used in the genetic analyses: Linkage group (LG)I, *mec-6(e1342)*; LGIII, *ced-4(n1162)*, *clp-1(tm690)*, *cnx-1(nr2009)*, *ced-9(n1950, n2812)*; LGIV, *itr-1(sa73)*, *ced-3(n2433)*; LGV, *crt-1(bz29)*, *unc-68(e540)*, *egl-1(n3082)*, *cyn-1(tm4171)*; and LGX, *asp-3(tm4559)*, *asp-4(ok2693)*. Detailed allele information is described in Wormbase (www.wormbase.org/). In addition to these strains, *bzIs8* is an integrated transgene located on LGX and contains a $P_{mec\text{-}4}$GFP construct, which directs GFP expression in six *C. elegans* touch receptor neurons (2). *smIs98* is an integrated transgene located on LGII and contains $P_{mec\text{-}3}$GFP and $P_{mec\text{-}7}$HBx constructs. *smIs3* is an integrated transgene containing $P_{mec\text{-}3}$GFP. *bzIs17* is an integrated transgene containing $P_{mec\text{-}4}$YC2.12, which directs expression of the YC2.12 cameleon calcium sensor under the control of the *mec-4* gene promoter (3). *smIs451* is an integrated transgene containing only $P_{mec\text{-}7}$HBx. All integrated transgenes were backcrossed six times with the N2 strain before being used for further genetic analyses.

Embryonic Lethality Assay. Gravid transgenic adults were placed on plates for 2 h at 20 °C to let them lay eggs. The plates were then heat-shocked at 33 °C for 1 h and returned to 20 °C for 1 h before removing all adult worms. After 24 h at 20 °C, the transgenic embryos were scored for embryonic lethality.

EMS Mutagenesis. EMS mutagenesis was carried out as described previously (1). Briefly, *smIs98*; *smEx*[P_{hsp}HBx + P_{hsp}GFP] L4 larvae were exposed to 47 mM EMS for 4 h with agitation. The F_1 progeny of mutagenized animals were cloned out, and the F_2 embryos were subjected to heat-shock treatment at 33 °C for 1 h and returned to 20 °C for 1 h. This heat-shock treatment was repeated three more times to ensure 100% killing of embryos by HBx. The surviving larvae with robust GFP expression in many cells were identified as putative suppressor mutants, which were subjected to the secondary screen using *smIs98*. Only those mutants in which HBx-induced touch cell death was completely or partially suppressed were considered as true suppressors and analyzed further.

Quantification of posterior lateral microtubule neuron (PLM) Killing by HBx. PLM neurons were scored in L4 larvae in the presence of the integrated transgene, *smIs98* or *bzIs8*, using a Nomarski microscope equipped with epifluorescence (4).

Transgenic Worms. Germ-line transformation was performed as described previously (5). The P_{hsp}HBx constructs (at 25 ng/μL each) were injected into animals with the appropriate genetic background, using $P_{sur\text{-}5}$GFP (25 ng/μL) as a coinjection marker, which directs GFP expression in all somatic cells in most developmental stages (6). The $P_{mec\text{-}7}$HBx construct (or its mutant derivatives) (25 ng/μL) was injected into *bzIs8*; *unc-76(e911)* animals, using p76-16B (5 ng/μL) as a coinjection marker, which rescues the Uncoordinated defect of the *unc-76(e911)* mutant. The $P_{mec\text{-}7}$CED-9, $P_{mec\text{-}7}$CED-9ΔTM, or $P_{mec\text{-}7}$hBcl-2 construct (25 ng/μL) was injected into *smIs98*; *ced-9(n1950)* animals, using pRF4 (50 ng/μL) as a coinjection marker, which causes a Roller phenotype in transgenic animals.

Molecular Biology. The HBx cDNA clone was kindly provided by Xiao-Kun Zhang (Burnham Institute for Medical Research, La Jolla, CA). Standard methods of cloning, sequencing, and PCR amplification were used. Briefly, full-length HBx cDNA was subcloned into the pGEX-4T-2 vector via its EcoRI and NotI sites to generate the pGEX-4T-2-HBx protein expression vector. To make P_{hsp}HBx constructs, full-length HBx cDNA was subcloned into *C. elegans* heat-shock vectors, pPD49.78 and pPD49.83, via NheI and KpnI sites. $P_{mec\text{-}7}$HBx was constructed by subcloning HBx cDNA into the pPD52.102 vector via its NheI and KpnI sites. The HBx mutant constructs containing G124L, I127A, E125A, or E126A substitutions were generated using a QuikChange Site-Directed Mutagenesis kit (Stratagene) and confirmed by DNA sequencing. To make Bcl-2, Bcl-xL, and Bax protein expression vectors, the coding regions for human Bcl-2 (1-218), human Bcl-xL(1-209), and mouse Bax(1-173) were amplified by PCR and subcloned into the pET-19b vector via its NdeI and XhoI sites, respectively. pET-24a-CED-9(68-251) and pET-24a-CED-9(68-251; G169E) were generated by Parrish et al. (7). $P_{mec\text{-}7}$CED-9 and $P_{mec\text{-}7}$hBcl-2 were generated by subcloning the full-length *ced-9* and human Bcl-2 cDNA fragments into the pPD52.102 vector via its NheI and EcoRV sites, respectively. $P_{mec\text{-}7}$CED-9ΔTM was generated by subcloning a cDNA fragment encoding CED-9 amino acids 1–251 into the pPD52.102 vector via its KpnI and EcoRV sites.

Protein Expression and Purification. GST-HBx proteins (wild type or mutants) were expressed in *Escherichia coli* strain BL21(DE3). The soluble fraction of the *E. coli* lysate was incubated with Glutathione Sepharose beads (Pharmacia) and purified GST-HBx proteins were eluted with 10 mM reduced glutathione (Amersham). CED-9(68-251), human Bcl-2(1-218), human Bcl-xL(1-209), and mouse Bax(1-173) proteins were expressed individually in BL21(DE3) as either a C-terminally or an N-terminally six-histidine–tagged protein, using a pET-24a or a pET-19b vector (Novagen), respectively. They were affinity purified using a Talon Metal Affinity Column (Clontech) and eluted with 250 mM imidazole.

GST Fusion Protein Pull-Down Assays. Purified GST-HBx proteins or GST protein (2.5 μg each) immobilized on Glutathione Sepharose beads (Pharmacia) were incubated with 5 μg of purified CED-9(68-251)-His_6, CED-9(68-251; G169E)-His_6, His_6-hBcl-2 (1-218), His_6-hBcl-xL(1-209), or His_6-mBax(1-173) in a binding buffer containing 25 mM Tris·HCl (pH 7.5), 150 mM NaCl, 0.1% Nonidet P-40, 10% glycerol, 1 mM phenylmethylsulphonyl fluoride, and 5 mM DTT at 4 °C for 2 h. One portion of the incubation mix was analyzed by Western blot to examine the input levels of GST-HBx proteins and Bcl-2 family proteins, using an antibody to GST (B-14) or the six-histidine tag (H15), respectively (Santa Cruz Biotechnology). The Sepharose beads were then washed five times with the same buffer before the bound proteins were resolved on a 15% SDS polyacrylamide gel and detected by immunoblotting.

Structural Modeling. Homology modeling of the complex structure between the HBx peptide (residues 120–128) and CED-9 was performed using the published complex structure between the EGL-1 Bcl-2 homology 3 (BH3) domain and CED-9 as a template (PDB ID code 1TY4). The model was further optimized using the program COOT manually to be reasonable (8). Both

modeling figures were created by the PyMOL program (9) and labeled using Adobe Illustrator CS4.

Chemical Treatment of *C. elegans*. We treated worms with chemicals, using an oil-base protocol described previously (10). Briefly, we first dissolved Thapsigargin (Sigma) or Cyclosporin A (Sigma) in DMSO and then diluted it in 100% soybean oil (Crisco). We placed L4 larval stage hermaphrodite animals onto standard NGM plates seeded with OP50. Oil solutions containing the chemicals were spread (0.8–1.0 mL) onto each plate so that the NGM surface was completely covered by oil. Worms lived at the interface of the NGM medium and the oil. We then examined their F_1 progeny for PLM cell death or the fluorescence-resonance energy transfer (FRET) ratio in PLMs.

Calcium Imaging and Analysis in *C. elegans*. A *C. elegans* strain with an integrated $P_{mec\text{-}4}$YC2.12 cameleon transgene (*bzIs17*) was used to quantify relative cytosolic calcium levels in PLM neurons (3). Animals at the L_1 larval stage were immobilized on a 2% agar pad in a solution containing 0.3 M 2,3-butanedione monoxime and 10 mM Hepes (pH 7.2). PLM neurons were visualized using an Axioplan 2 Nomarski Microscope (Zeiss) equipped with a SensiCam CCD camera (PCO Imaging). CFP (427/10–25 excitation, 440 dichroic, 472/30–25 emission), YFP (504/12–25 excitation, 520 dichroic, 542/27–25 emission), and FRET (427/10–25 excitation, 440 dichroic, 542/27–25 emission) filters (Semrock); a colliminating emission port adapter (Photometrics); and the Slidebook 5.0 software (Intelligent Imaging Innovations) were used to collect FRET data. The CFP channel collects CFP emission after CFP excitation and the FRET channel collects YFP emission after CFP excitation. Analysis of exported tiff files containing data from the FRET or CFP channel was performed using the ImageJ software (National Institutes of Health). The FRET ratio was calculated by $(FRET_{PLM} - FRET_{bkgnd})/(CFP_{PLM} - CFP_{bkgnd})$, where $FRET_{PLM}$ and CFP_{PLM} are the mean fluorescent intensities in the FRET and CFP channels of the PLM neuron and $FRET_{bkgnd}$ and CFP_{bkgnd} are the mean fluorescent intensities in the FRET and CFP channels of a background region adjacent to the PLM neurons (11, 12).

Statistical Analysis. Experimental data are presented as mean ± SEM. Significance of the differences between two datasets was determined using Student's *t* test.

1. Brenner S (1974) The genetics of Caenorhabditis elegans. *Genetics* 77(1):71–94.
2. Harbinder S, et al. (1997) Genetically targeted cell disruption in Caenorhabditis elegans. *Proc Natl Acad Sci USA* 94(24):13128–13133.
3. Suzuki H, et al. (2003) In vivo imaging of C. elegans mechanosensory neurons demonstrates a specific role for the MEC-4 channel in the process of gentle touch sensation. *Neuron* 39(6):1005–1017.
4. Geng X, et al. (2008) Inhibition of CED-3 zymogen activation and apoptosis in Caenorhabditis elegans by caspase homolog CSP-3. *Nat Struct Mol Biol* 15(10):1094–1101.
5. Geng X, et al. (2009) Caenorhabditis elegans caspase homolog CSP-2 inhibits CED-3 autoactivation and apoptosis in germ cells. *Cell Death Differ* 16(10):1385–1394.
6. Gu T, Orita S, Han M (1998) Caenorhabditis elegans SUR-5, a novel but conserved protein, negatively regulates LET-60 Ras activity during vulval induction. *Mol Cell Biol* 18(8):4556–4564.
7. Parrish J, Metters H, Chen L, Xue D (2000) Demonstration of the in vivo interaction of key cell death regulators by structure-based design of second-site suppressors. *Proc Natl Acad Sci USA* 97(22):11916–11921.
8. Emsley P, Cowtan K (2004) Coot: Model-building tools for molecular graphics. *Acta Crystallogr D Biol Crystallogr* 60(Pt 12 Pt 1):2126–2132.
9. DeLano W (2002) *The PyMOL Molecular Graphics System* (DeLano Scientific, San Carlos, CA).
10. Kokel D, Li Y, Qin J, Xue D (2006) The nongenotoxic carcinogens naphthalene and para-dichlorobenzene suppress apoptosis in Caenorhabditis elegans. *Nat Chem Biol* 2(6):338–345.
11. Vanderklish PW, et al. (2000) Marking synaptic activity in dendritic spines with a calpain substrate exhibiting fluorescence resonance energy transfer. *Proc Natl Acad Sci USA* 97(5):2253–2258.
12. Palmer AE, Tsien RY (2006) Measuring calcium signaling using genetically targetable fluorescent indicators. *Nat Protoc* 1(3):1057–1065.

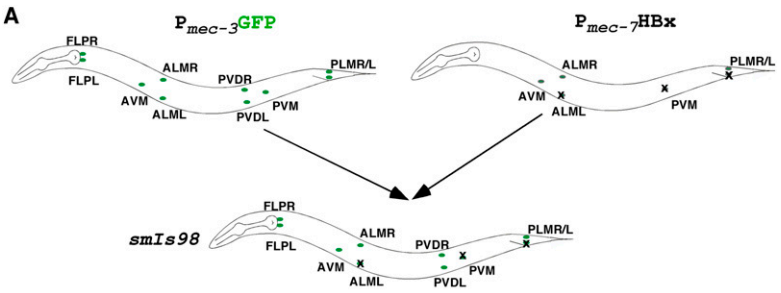

B

Genotype	% cell missing					
	AVM	ALM	PVM	PLM	FLP	PVD
smIs3[P_{mec-3}GFP]	0%	0%	1%	0%	0%	0%
smIs98[P_{mec-7}HBx+P_{mec-3}GFP]	14%	13%	20%	50%	0%	0%

C

Genotype	% PLM Missing
smIs98	50%
smIs98; cyn-1(tm4171)	17%
smIs98 + DMSO	50%
smIs98 + CsA	15%
smIs98; ced-3(n2433) + DMSO	24%
smIs98; ced-3(n2433) + CsA	4%
smIs98; mec-6(e1342) + DMSO	10%
smIs98; mec-6(e1342) + CsA	10%
smIs98; clp-1(tm690) + DMSO	14%
smIs98; clp-1(tm690) + CsA	11%

Fig. S1. Expression of HBx in touch cells induces ectopic neuronal cell death, which can be suppressed by cyclosporin A (CsA). (*A*) Generation of the *smIs98* strain. P_{mec-3}GFP directs GFP expression in ten sensory neurons (indicated by green circles). P_{mec-7}HBx directs HBx expression in six of the ten neurons, leading to the death of some of these neurons (indicated by "X"). An integrated transgene (*smIs98*) carrying both P_{mec-3}GFP and P_{mec-7}HBx resulted in loss of touch cells, which is shown in *B*. Six mechanosensory neurons are anterior lateral microtubule neurons at the left and right (ALML and ALMR), anterior ventral microtubule neuron (AVM), posterior ventral microtubule neuron (PVM), and PLML and PLMR. (*B*) Ectopic neuronal death caused by expression of HBx in six touch cells. *smIs3* is an integrated transgene carrying only P_{mec-3}GFP. The percentage of cells killed by HBx in each neuronal cell type was shown. At least 500 L4 stage larvae were scored in each strain. (*C*) Inhibition of HBx-induced cell death by CsA. The percentage of PLM death in animals treated with 1 mM CsA was scored as described in Fig. 2*A*. At least 100 L4 stage larvae from each strain were scored.

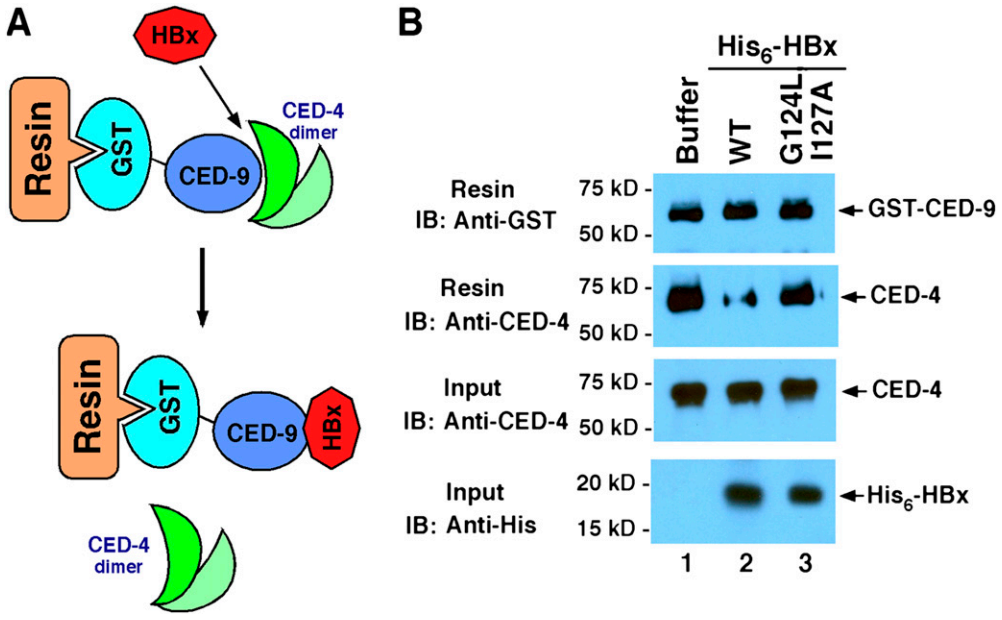

Fig. S2. HBx releases CED-4 from the CED-4/CED-9 complex. (*A*) A schematic diagram of the CED-4–releasing assay. (*B*) Five hundred nanograms of wild-type or mutant six-histidine–tagged HBx proteins was added to GST-CED-9/CED-4 complexes immobilized on Glutathione Sepharose resins and incubated at 4 °C for 2 h. One portion of the incubation mix was analyzed by immunoblotting (IB) to examine the input levels of CED-4 and His_6-HBx proteins. The remaining resins were washed with binding buffer several times and the amount of CED-4 still complexing with GST-CED-9 on the resins was analyzed by immunoblotting, using an anti-CED-4 antibody.

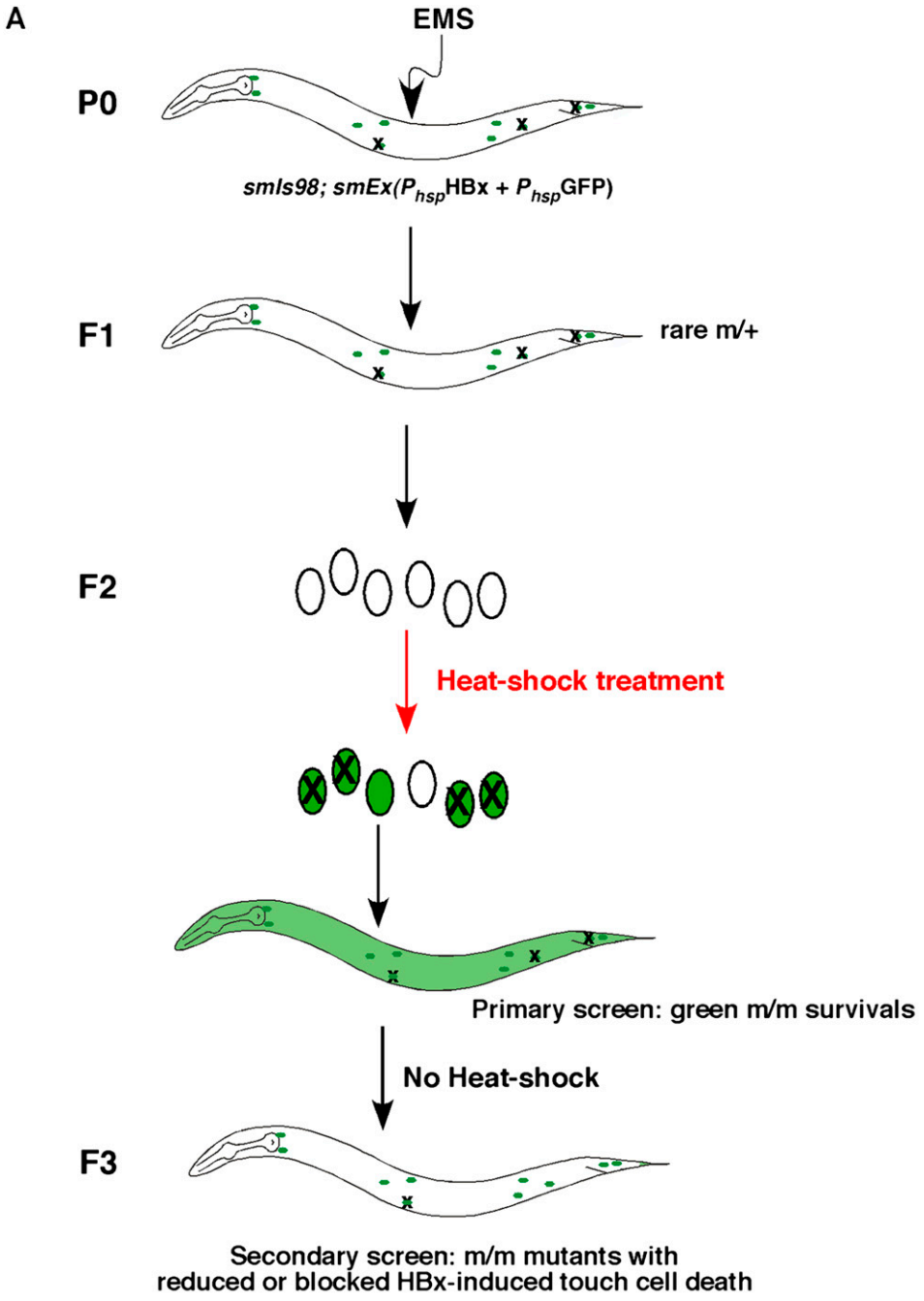

B

Genotype	Missing PLM (%)	Amino Acid change	Nucleotide change
smIs98	50%		
smIs98; mec-6(sm221)	18%	$Gly^{77} \rightarrow Ser$	GGT→AGT
smIs98; clp-1(sm250)	14%	$Trp^{295} \rightarrow Opal$	TGG→TGA
smIs98; ced-4(sm224)	23%	$Glu^{383} \rightarrow Ochre$	GAA→TAA

Fig. S3. Identification of cellular effectors or targets of HBx through an HBx suppressor screen. (*A*) Strategy of isolating suppressors of HBx-induced cell death (*hids*) in *C. elegans*. *smIs98* animals carrying both P_{hsp}HBx and P_{hsp}GFP were mutagenized by ethyl methanesulfonate (EMS). Embryos from the second generation of mutagenized animals were treated with heat shock. GFP-expressing animals that survived the heat-shock treatment were selected ("X" indicates dying embryos) and analyzed further for suppression of PLM death, using *smIs98*. Only those mutants that displayed significant suppression of PLM death are considered as true *hids* mutants. (*B*) Characterization of three *hids* mutants. *sm221*, *sm224*, and *sm250* were found to affect *mec-6*, *ced-4*, and *clp-1*, respectively. The nature of the amino acid and nucleotide changes is indicated (nucleotide changes are underlined). At least 200 L4 larvae from each suppressor strain were scored for PLM death.